Exp. Theo. NANOTECHNOLOGY 3 (2019) 229-237

Experimental and Theoretical
NANOTECHNOLOGY
http://etn.siats.co.uk/

Optical and structural properties of zinc oxide nanocrystalline

C. Tedlle[1,*], *N. Chen*[1], *I. Pero*[2]

[1]Department of Electrical Engineering and Computer Science, South Dakota State University, Brooking, SD 57007, USA

[2]Centre for Mechanical Technology and Automation, Department of Mechanical Engineering, University of Aveiro, 3810-193 Aveiro, Portugal

*) Email: qihua.fan@sdstate.edu

Received: 2/2/2018 / *Accepted:* 24/7/2018 / *Published:* 1/9/2019

Abstract: Zinc oxide (ZnO) is a wide band gap (~3.37 eV) semiconductor. Thin film ZnO has many attractive applications in optoelectronics and sensors. Recently, nanostructured ZnO (e.g. ZnO quantum dot) has been demonstrated as a hyperbolic material; its dielectric function has opposite signs along different crystal axes within the mid-infrared, making it an interesting material for metamaterials and nanophotonics. Conventional sputtering deposition usually leads to the formation of polycrystalline ZnO films with randomly oriented grains and rough surface. This work demonstrated a solution-based process to grow ZnO thin films with highly oriented nanocrystals. Low-temperature plasmas were employed to modulate the microstructure and optical properties of the films. Such highly anisotropic nanostructured transparent semiconductor films may lead to interesting material properties in developing new optoelectronic devices.

Keywords: ZnO, Sol-gel, oxygen plasma, crystal size.

1. NTRODUCTION

Zinc oxide (ZnO) is a II–VI compound semiconductor with wide band gap ~3.37 eV [1, 2]. Thin film ZnO is highly transparent in the visible spectrum (>90%), with moderate Hall mobility ranging from 0.2 to 7 $cm^2V^{-1}s^{-1}$. These characteristics combined with other interesting properties, such as a strong blue luminescence and a large acoustic velocity (6336 m/s), make ZnO attractive for use in many applications. Owing to their better stability than

indium tin oxide in hydrogen plasma, ZnO thin films have been used in the fabrication of hydrogenated amorphous silicon solar cells [3, 4]. ZnO has also been used as transparent electrodes in displays and piezoelectric devices [5-7]. Wide band gap ZnO is a potential material for short-wavelength optoelectronic devices, such as UV lasers, blue to UV light-emitting diodes and UV detectors [8, 9], which can be applied to high density data storage systems, solid-state lighting, secure communications and bio-detection. Of particularly interesting, ZnO nanostructures (e.g. ZnO quantum dots) have been demonstrated as a hyperbolic material; its dielectric function has opposite signs along different crystal axes within the mid- infrared, making it an attractive metamaterial and promising for nanophotonics [10].

The wurtzite crystal structure of ZnO is thermodynamically stable with oxygen atoms on hexagonal sites and zinc atoms on tetrahedral sites [11]. It exists with non-polar (1011) surface termination, polar (0001) O-termination, and polar (0001) Zn-terminated surfaces [12], resulting in termination- dependent chemical reactivity. ZnO crystallites with preferential orientation are desirable for applications where crystallographic anisotropy is a prerequisite as in UV-diode, piezoelectric surface acoustic wave or acousto-optic devices [13]. Various methods have been used to fabricate ZnO films. The common methods include pulsed laser deposition, RF magnetron sputtering, chemical vapor deposition, and spray pyrolysis [14, 15]. Polycrystalline ZnO films fabricated from these processes usually consist of randomly oriented crystals. Furthermore, vacuum-based processes are generally expensive. Solution-based sol-gel method offers simple, easy and low- cost deposition of ZnO, which can be integrated into roll-to-roll fabrication [16-18]. ZnO films prepared by solution processes usually have high resistivity. Post annealing at moderate temperatures in a proper environment is needed to reduce the resistivity.

This work aims to produce nanostructured ZnO thin films with highly oriented crystals using a solution-based process. As discussed above, such films may find a broad variety of applications. Post plasma treatment is employed to verify whether or not it can modulate the film structures and optical properties at low temperatures.

Exp. Theo. NANOTECHNOLOGY 3 (2019) 229-237

2. EXPERIMENTAL PROCEDURE

ZnO nanostructured thin films were deposited by sol-gel spin coating onto glass substrate. Zinc acetate [$Zn(CH_3COO)- 2H_2O$],2-methoxethanol (MEA), and ethanolamine were used as the starting material, solvent, and stabilizer, respectively. The molar ratio of MEA to zinc acetate dehydrate was maintained at 1.0 and the concentration of zinc acetate was 0.35 M. The solution was stirred at 500 RPM for two hours at room temperature followed by stirring at 80^{o} C for 1 hr to result in a clear homogeneous solution. The glass substrates were cleaned with a soapy water, DI water, acetone and IPA in sequence using a Fisher Scientific FS60D ultrasonic cleaner, each step for 10 min, respectively. The zinc oxide solution was then spin-coated on the glass substrates at 2500 RPM for 30 seconds using a LAURELL WS-650MH- 23NPP/LITE spin coater. After the deposition, the film was dried at different temperatures from 200^{o} C to 500^{o} C for 1 hour in a furnace to remove organic residuals. The routine was repeated from coating to drying for five times to give a final film thickness ~200 nm.

After the films were deposited, the samples were processed with oxygen plasma generated with a capacitively coupled RF discharge, during which the oxygen gas pressure was maintained at ~2 Torr. No external heating was applied and the substrate temperature was below 150^{o} C during the plasma treatment. The thickness of the film was measured using VEECO DEKTAK 150 surface profiler. The transmittance measurement was carried out using FILMETRICS F20-UVX spectrophotometer. X-ray diffraction (XRD) was taken using RIGAKU SMARTLAB system.

3. RESULTS AND DISCUSSION

The transmission spectra of the ZnO films fabricated at different temperatures are shown in Figure **1**. The ZnO film prepared at 200^{o}C showed good transmittance in 380-750nm range with an average transmittance above 90%. Increasing the temperature from 200^{o}C to 400^{o}C, the transmittance increased slightly. The maximum point of transmittance shifted to shorter wavelength with the increase in the temperature, indicating that the film optical thickness was

Exp. Theo. NANOTECHNOLOGY 3 (2019) 229-237

reduced. This was due to the removal of organic residuals at higher temperatures. Further increase the fabrication temperature to 500^{o} C led to decrease in the transmittance. Two possible reasons contributed to this reduction in transparency: surface roughening that led to light scattering and oxygen loss that created vacancies at high temperatures. Similar reduction in optical transparency was observed when the annealing temperature of ZnO films was increased [19].

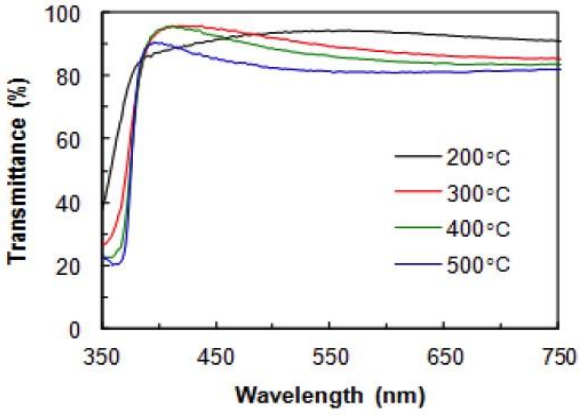

Figure 1: Optical transmittance spectra of ZnO films prepared at different temperature.

Figure **2** shows the XRD pattern of the ZnO films prepared at different temperatures. The ZnO films prepared at temperatures above 400^{o}C showed oriented crystal growth along (002) plane. This oriented growth confirmed that the highest density of Zn atoms was in the (002) planes as it was kinetically favorable [20]. At sufficient temperatures, the excess energy acquired by the ZnO crystallites allowed them to orient themselves along the (002) plane where the surface energy was minimum [19]. The ZnO films prepared at temperatures below 300^{o}C did not exhibit obvious crystallization. The films were mostly amorphous. An increase in the (002) peak intensity was observed when the films were prepared at 300^{o}C, 400^{o}C, and 500^{o}C, as shown in Figure **2**. The gain in peak intensity was obviously due to an increase in the crystallinity with temperature.

Exp. Theo. NANOTECHNOLOGY 3 (2019) 229-237

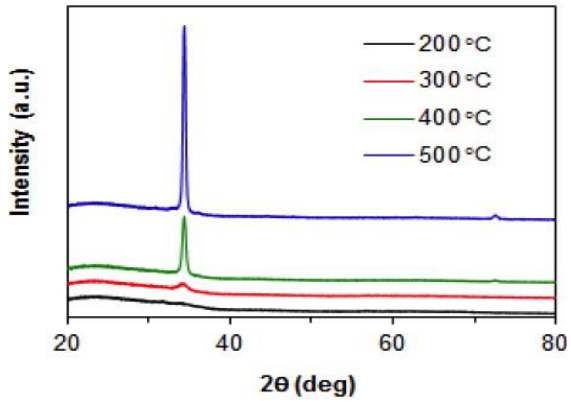

Figure 2: XRD patterns of ZnO films prepared at different temperatures.

Figure **3** shows the effect of temperature on the crystal size of the ZnO films. The average crystal size increased with the process temperature. The size of crystallite was estimated from the full-width at half-maximum (FWHM) of (002) peak using the Scherrer formula [21]. The crystal size increased from 5.9 nm at 300^{O}C to 23.8 nm at 500^{O}C. The increase in the temperature caused coalescence/merging of small grains by grain boundary diffusion, resulting in grain growth [22].

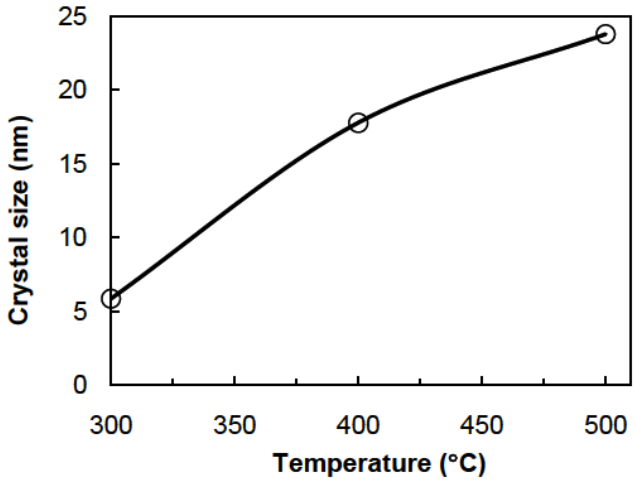

Figure 3: Effect of temperature on the crystal size of the ZnO films.

Figure **4** compares the optical transmittance of the ZnO films prepared at 500^{O}C followed by

Exp. Theo. NANOTECHNOLOGY 3 (2019) 229-237

oxygen plasma treatment for

5, 10, 20 and 40 minutes. Overall, the transmittance slightly increased after the plasma treatment. 20-minute oxygen plasma treatment appeared sufficient, while prolonged plasma treatment (e.g. 40 minutes) led to slight decreasein the transmittance. The variation in the transmittance with the plasma treatment time was attributed to two opposite effects:
1) oxygen plasma reduced oxygen vacancies and led to the increase in the transmittance; and
2) the bombardment of charged ions on the ZnO film created defects and roughened the film surface, leading to a decrease in the transmittance.

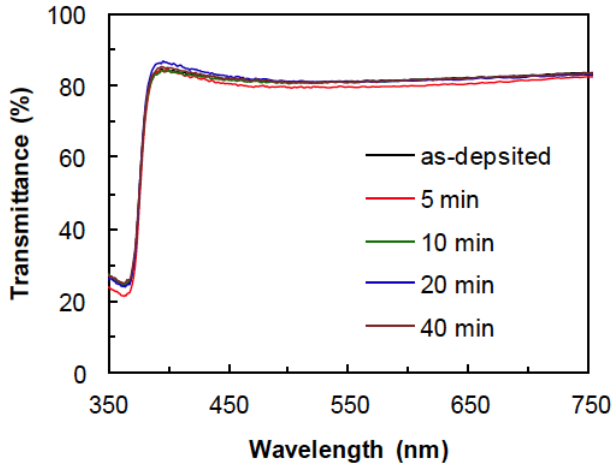

Figure 4: Comparison of optical transmission spectra of ZnO films processed at 500^{O}C followed by oxygen plasma treatment for different times.

Figure **5** compares XRD spectra of the ZnO films processed at 500^{O}C followed by oxygen plasma treatment for 5, 10, 20

and 40 minutes. The FWHM values for the XRD spectra are presented in Table **1**. The FWHM value for the as-deposited ZnO film was 0.3639, while the lowest FWHM value was obtained for 20 min O2 plasma treatment. However, sharpening of the diffraction peak or lowering of the FWHM value was not seen in the films exposed to O2 plasma beyond 20 minutes. This result was further supported by analyzing the crystal size of the ZnO films treated by O2 plasma for different time.

Exp. Theo. NANOTECHNOLOGY 3 (2019) 229-237

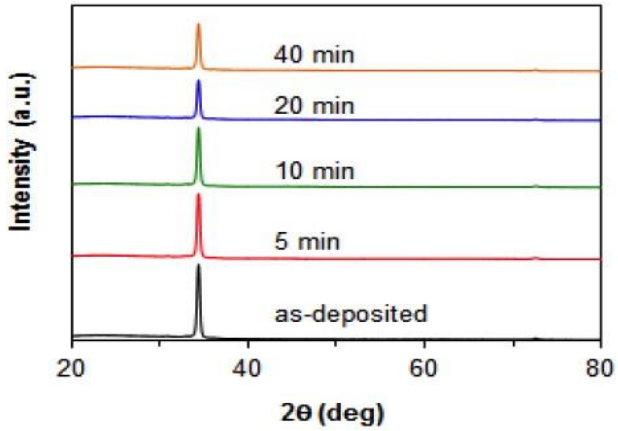

Figure 5: Comparison of XRD spectra of ZnO films processed at 500^{O}C followed by oxygen plasma treatment for different times.

Table 1: FWHM of XRD (002) Peak for the ZnO Films Treated with O_2 Plasma

O_2 Plasma Treatment	**FWHM**
As-deposited	0.3639
5 min	0.3585
10 min	0.3603
20 min	0.3567
40 min	0.3652

Figure **6** shows the crystal size of the ZnO films treated by oxygen plasma. The average crystal size increased slightly with plasma treatment time till 20 minutes, after which the crystal size decreased. The crystal size increased from 23.80 nm (as-deposited) to 24.35 nm (20-minute oxygen plasma). The crystal size after 40-minute oxygen plasma treatment dropped to 23.77 nm. These results indicated that oxygen plasma treatment increased the crystallinity of the ZnO films by increasing the size of the crystallites. An optimum treatment time was 20 minutes. This result was in agreement with the transmittance variation. As discussed previously, this happened due to the diffusion of oxygen from the plasma into the ZnO film and reduced oxygen vacancies. However, further increase in oxygen plasma treatment time led to excessive ion bombardment, which broke ZnO bonds.

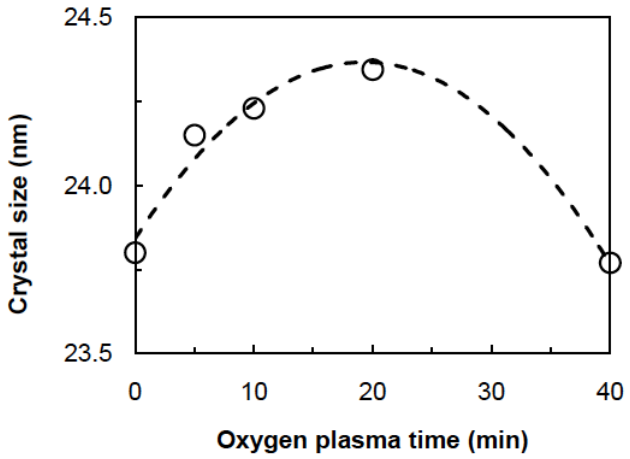

Figure 6: Effects of oxygen plasma treatment time on the crystal size of ZnO films.

4. CONCLUSIONS

Highly oriented (002) ZnO nanocrystalline thin films was produced by a solution-based process. The crystallinity of the ZnO films increased with the process temperature. The transmittance decreased slightly as the process temperature approached 500^{o} C. Oxygen plasma treatment led to increased transmittance. However, prolonged oxygen plasma treatment led to reduced transmittance. The variation in the transmittance was in agreement with the change in the crystal size deduced from the FWHM of the XRD (002) peak.

REFERENCES

[1] Yasser A. Abdel-Hadi, Exp. Theo. NANOTECHNOLOGY 2 (2018) 61
[2] Meena JS, Chu M-C, Chang Y-C, J Mater Chem C 1 (2013) 6613
[3] Li H, Wang J, Liu H, Vacuum 77 (2004) 57
[4] Zhou Z, Kato K, Komaki T, J Eur Ceram Soc 24 (2004) 139
[5] Wang D, Zhao D, Wang F, Yao B, Shen D. Physica Status Solidi A 212 (2015) 846
[6] Van de Walle CG. Phys Rev Lett 85 (2000) 1012
[7] Kumar NS, Bangera KV, Shivakumar G. Appl Nanosci 4 (2014) 209
[8] Ozgur U, Hofstetter D, Morkoc H. Proc IEEE 98 (2010) 1255
[9] Znaidi L. Mater Sci Eng B 174 (2010) 18
[10] Fonoberov VA, Balandin AA. J Phys Condens Matter 17 (2005) 1085
[11] Hsu C-W, Cheng T-C, Yang C-H, Shen Y-L, Wu J-S, Wu S-Y. J Alloys Comp. 509 (2011) 1774
[12] Kuo F-L, Li Y, Solomon M, Du J, Shepherd ND. J Phys D Appl Phys 45 (2012) 065301
[13] Znaidi L. Materi Sci Eng B 174 (2010) 18
[14] Elilarassi R, Chandrasekaran G. Mater Chem Phys 121 (2010) 378

[15] Ng Z-N, Chan K-Y, Sin Y-K, Hoon J-W, Ng S-S. Ceram Int 39 (2013) S263
[16] Sengupta J, Sahoo R, Mukherjee C. Mater Lett 83 (2012) 84
[17] Ng Z-N, Chan K-Y, Tohsophon T. Appl Surf Sci 258 (2012) 9604
[18] Zak AK, Abrishami ME, Majid WA, Yousefi R, Hosseini S. Ceram Int 37 (2011) 393
[19] Sengupta J, Sahoo R, Bardhan K, Mukherjee C. Mater Lett 65 (2011) 2572
[20] Zhai J, Zhang L, Yao X. Ceram Int 26 (2000) 883
[21] Chen X, Zhou J, Wang H, Xu P, Pan G. Chinese Phys B 20 (2011) 096102
[22] Caglar Y, Ilican S, Caglar M, J Alloys Comp. 481 (2009) 885

Exp. Theo. NANOTECHNOLOGY 3 (2019) 229-237